RASĀYAN *J. Chem.*
Vol. 18 | No. 2 |913-918| April - June | 2025
ISSN: 0974-1496 | e-ISSN: 0976-0083 | CODEN: RJCABP
http://www.rasayanjournal.com
http://www.rasayanjournal.co.in

HYDROTHERMAL FABRICATION OF Z-SCHEME $Sn_3O_4/BiVO_4$ NANOCOMPOSITE FOR PHOTOCATALYTIC DEGRADATION OF RHODAMINE B DYE

Mohammad Farhan[1], Anil Kumar Singh[1] and Gandharve Kumar[2,✉]
[1]Department of Chemistry, Faculty of Engineering, Teerthanker Mahaveer University, Moradabad- 244001, Uttar Pradesh, India
[2]Department of Chemistry, School of Basic Sciences, Galgotias University, Greater Noida- 203201, Uttar Pradesh, India.
✉Corresponding author: gandharve.kumar@galgotiasuniversity.edu.in

ABSTRACT
$Sn_3O_4/BiVO_4$ photocatalyst was prepared by the hydrothermal route, and its activity was tested on the degradation of RhB dye under sunlight. The 15 wt% $Sn_3O_4/BiVO_4$ photocatalysts degraded 99 % (RhB, 10 mg/L), whose degradation rate was 5.7 times and 10 times superior to $BiVO_4$ and Sn_3O_4 photocatalysts, respectively. The strong visible light absorption by 15 wt% $Sn_3O_4/BiVO_4$ nanocomposite, band position of Sn_3O_4 and $BiVO_4$, which are like Z-scheme, proficient suppression of electron-hole recombination, and formation of reactive oxygen species *in situ* are the main reasons for the better photocatalytic efficiency of $Sn_3O_4/BiVO_4$ nanocomposite.
Keywords: Z-Scheme, Sn_3O_4, $BiVO_4$, Solar Photocatalyst, Degradation.
RASĀYAN *J. Chem.*, Vol. 18, No.2, 2025

INTRODUCTION

Dyes are an important class of organic chemicals that are used extensively in many different sectors, such as leather, plastics, food, paper, textiles, cosmetics, and medicines.[1,2] These dye pollutants severely affect aquatic ecosystems by obstructing sunlight penetration, reducing photosynthesis, and depleting dissolved oxygen levels, which can disrupt aquatic life.[3–5] Conventional wastewater treatment methods, such as chemical coagulation, adsorption, and biological processes, are often inadequate for complete dye removal. These methods are energy-intensive, costly, and may generate secondary pollutants, merely transferring contaminants from one phase to another.[6,7] Photocatalytic degradation has emerged as a promising alternative for dye remediation, offering a sustainable and efficient solution. This process involves using a photocatalyst to harness light energy, driving chemical reactions that degrade complex dye molecules into harmless compounds like carbon dioxide and water. The effectiveness of photocatalysis depends on the properties of the photocatalyst, including its ability to absorb visible light, separate charge carriers, and prevent electron-hole recombination.[8–10] $BiVO_4$, with its simplest ternary oxide semiconductor, exhibits a narrow bandgap of 2.4–2.5 eV, enabling efficient visible-light absorption. The stratified architecture also promotes the segregation and conveyance of photogenerated charge carriers, hence improving photocatalytic efficacy. However, $BiVO_4$ has limitations, including rapid electron-hole recombination and low quantum yield, which reduce its overall efficiency.

To overcome these drawbacks, the development of Z-scheme type heterojunctions along with semiconductors consisting compatible band edges concerning $BiVO_4$.[11–13] The development of a Z-scheme heterojunction composite is valuable from a photocatalytic perspective as it reduces the charge carrier recombination rate and comprises robust redox capabilities.[14–16] Yong *et al.* developed a Z-scheme $In_2S_3/BiVO_4$ photocatalyst, which demonstrates enhanced photocatalytic activity towards the glyphosate photodegradation.[17] Luo *et al.* synthesized a $MoSe_2/BiVO_4$ heterojunction with Z-scheme, which demonstrates superior photocatalytic potential toward the photocatalytic eradication of glyphosate.[18] Similarly, Chen *et al.* designed a novel $AgI/BiVO_4$ photocatalyst with a Z-scheme heterojunction, which effectively removes the tetracycline.[19] Herein, we developed a novel $Sn_3O_4/BiVO_4$ heterostructure *via* a two-step hydrothermal process. The plausible development of a Z-scheme type heterostructure among

http://doi.org/10.31788/RJC.2025.1829245

Sn_3O_4 and $BiVO_4$ has been outlined. The $Sn_3O_4/BiVO_4$ nanocomposite exhibited excellent degradation efficiency towards the removal of rhodamine B dye under exposure to natural sunlight.

EXPERIMENTAL

Chemicals Used

All chemicals used in this work were purchased from Rankem Pvt. Ltd., India. Stannous chloride dihydrate, bismuth nitrate pentahydrate, ammonium meta vanadate, tri-sodium citrate, ethylene glycol, isopropyl alcohol, chloroform, and ammonium oxalate, Rhodamine B dye were procured from Rankem Pvt. Ltd., India.

Synthesis of Sn_3O_4 Nanoflakes

Firstly, the Hydrothermal method was used for the preparation of Sn_3O_4 nanoflakes. Solution A was obtained by adding 0.1 g of NaOH in 12.5 mL deionized water, which was added dropwise into solution B comprising 4 mmol $SnCl_2.2H_2O$ and 12.5 mmol tri-sodium citrate dihydrate in 12.5 mL deionized water, and stirred for 0.5h. The final mixture was put into a steel autoclave at 200°C in an oven for 12h. Finally, the supernatant liquid was disposed of, and the final product was gathered, cleaned with water and ethanol, and then left to dry overnight at 50 °C.

Synthesis of $Sn_3O_4/BiVO_4$ Photocatalyst

The hydrothermal method was used for the preparation of $Sn_3O_4/BiVO_4$ nanocomposites. 2 mmol NH_4VO_3 and 2 millimoles of Bismuth nitrate pentahydrate were mixed in 50 milliliters of DI water, and the final solution was mixed for 0.5h. The solution pH was maintained at 6 using 10 M NaOH. Then, a certain amount of Sn_3O_4 (10, 15, and 20 wt.%) was added to it, and the final solution was allowed to mix for 1 h. At last, the final solution was put into an autoclave (Teflon-lined) and heated for about 24 h at 180 °C. The prepared batches of $Sn_3O_4/BiVO_4$ nanocomposites were separated and dried at 60 °C overnight.

RESULTS AND DISCUSSION

The degradation studies were conducted on 10 ppm RhB dye by $Sn_3O_4/BiVO_4$ nanocomposites dispersed in aqueous solution in the presence of sunlight. Photocatalytic degradation experiments were conducted at Teerthanker Mahaveer University, Moradabad, India, in June and July month of 2024. Initially, for, first 60 min, the dark study was performed to ensure adsorption or desorption equilibrium. Then, the beaker containing the reaction mixture was placed under sunlight to conduct the degradation studies. At regular time intervals, 1 ml of aliquots was taken during photoreaction, followed by centrifugation to separate the photocatalyst. At last, the change in intensity of RhB dye was observed. The phase composition of 15 wt% $Sn_3O_4/BiVO_4$, along with respective individual pristine components, e.g., Sn_3O_4 and $BiVO_4$, was analyzed by the XRD method, and the results are presented in Fig.-1a. The pristine $BiVO_4$ and Sn_3O_4 exhibit XRD patterns that are consistent with monoclinic scheelite phase (JCPDS No. 14-0688) and triclinic phases (JCPDS No. 16- 0737), respectively.[20,21] The characteristic diffraction peak of Sn_3O_4 was observed in the best-performing photocatalyst, 15 wt% $Sn_3O_4/BiVO_4$. The microstructures and sizes of pristine batches of Sn_3O_4 and $BiVO_4$, and 15 wt% $Sn_3O_4/BiVO_4$ heterostructure were explored by Scanning electron microscopy (SEM). The scanning electron microscopy image of Sn_3O_4 discloses the development of nanoflakes of non-uniform sizes diameters ranging from 100-300 nm (Fig.-1b). While the scanning electron microscopy image of $BiVO_4$ displayed non-uniform nanoplate-like structures of dimensions ranging between 300-600 nm (Fig.-1c).

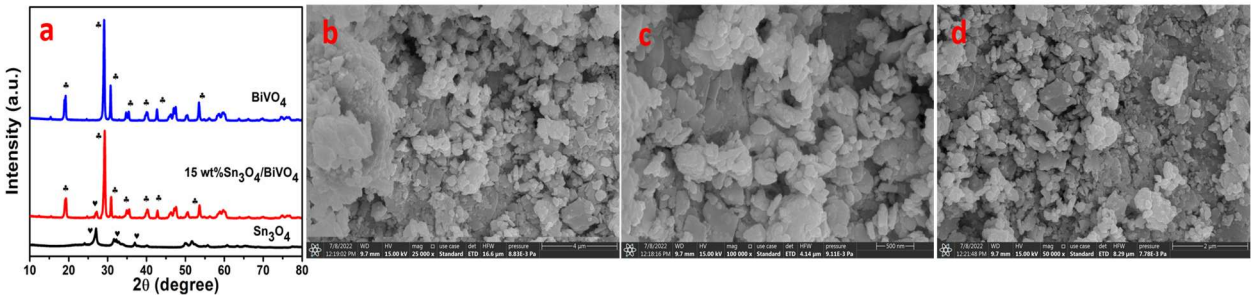

Fig.-1: (a) XRD and SEM of $BiVO_4$, Sn_3O_4, and 15 wt% $Sn_3O_4/BiVO_4$ Nanocomposite

The FESEM image of 15 wt% $Sn_3O_4/BiVO_4$ revealed nanoflakes of Sn_3O_4 adhered to the surface of $BiVO_4$, which appears like a nanoplate morphology (Fig.-1d). The size, morphology, and hierarchical structure of $Sn_3O_4/BiVO_4$ were retained as pristine $BiVO_4$.

The UV-vis DRS studies were utilized for the determination of the band gap of 15 wt% $Sn_3O_4/BiVO_4$, along with Sn_3O_4 and $BiVO_4$. Figure-2a discloses that pristine $BiVO_4$ and the $Sn_3O_4/BiVO_4$ strongly absorb in the UV region, expanding to the visible light region, whereas Sn_3O_4 absorbs solely in the visible region, as represented in Fig.-2a. Tauc's Plot $(\alpha h\nu)^2$ versus $h\nu$ (eV) is shown in Fig.-2b. The band gap energies of Sn_3O_4, $BiVO_4$, and 15 wt% $Sn_3O_4/BiVO_4$ are determined as 2.85 electron volt, 2.39 electron volt, and 2.46 electron volt (Fig.-2b). The value of conduction and valence band was calculated by using an equation, (EVB= χ- Ee+1/2Eg) and (ECB= EVB–Eg). ECB represents the energy of the conduction band and EVB shows the energy of the valence band, and Eg represents the band gap energy. The χ values for Sn_3O_4 and $BiVO_4$ are 5.44 eV and 6.19 eV for respectively, and Ee (Energy of free electron). The ECB and EVB values of $BiVO_4$ are 0.49 electron Volt and 2.88 electron Volt. Similarly, the value of conduction band (ECB) and valence band (EVB) of Sn_3O_4 are -0.49 electron Volt and 2.36 electron Volt.

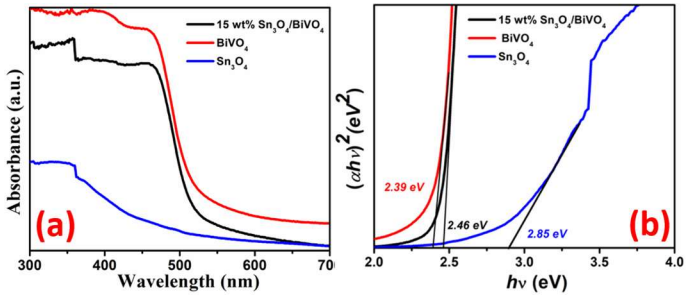

Fig.-2: (a) Absorption Spectra, (b) The Relative Band Gap Energy of Sn_3O_4, $BiVO_4$, and 15 wt% $Sn_3O_4/BiVO_4$

Photocatalyst Performance Study

The UV-visible absorbance spectra of 10mg/L of RhB treated with a photocatalyst dose of 60mg/100mL, under dark conditions and followed by visible light exposure, are given in Fig.-3a. The Fig.-3b shows the plot of C_t/C_0 versus time(t). The data corresponding to the photocatalytic degradation under visible light is fitted linearly with first-order kinetics as shown in Fig.-3c. The photolysis, i.e., RhB without treating with the photocatalyst, is negligible (Fig.-3b, Table-1). The optimization of photocatalyst dosage and RhB concentration is mentioned in Fig.-4. The results of degradation rate for different batches of $Sn_3O_4/BiVO_4$, Sn_3O_4, and $BiVO_4$ are shown in Table-1. The batch 15 wt% $Sn_3O_4/BiVO_4$ exhibited maximum photocatalytic efficiency, i.e., 99 % RhB degradation in 60 min of sunlight irradiation, which was 6.0 times higher than the pristine $BiVO_4$ as a photocatalyst. The corresponding rate of degradation by 15 wt% $Sn_3O_4/BiVO_4$ was 0.040 min^{-1} for RhB. The photocatalytic degradation of pristine Sn_3O_4 and $BiVO_4$ was evaluated as 0.004 and 0.007 min^{-1}, respectively, under the same conditions. The enhanced degradation of RhB by 15 wt% $Sn_3O_4/BiVO_4$ is because of the formation of ROS. This has been ascertained from specific ROS scavenging studies (Fig.-3d). The batches of RhB solution treated with 15 wt% $Sn_3O_4/BiVO_4$ were treated with ROS scavengers, e.g., isopropyl alcohol, chloroform, and ammonium oxalate[22], as h^+, $O_2^{-\bullet}$, and •OH quenchers respectively. Among the ROS scavengers, the batch treated with chloroform exhibited a profound decrease in the photocatalytic degradation rate.

Table-1: Photocatalytic Degradation Experiments Summary

Sample name	Adsorption %	Degradation %	K (min^{-1})	R^2
20 wt% $Sn_3O_4/BiVO_4$	24%	80%	0.023	0.993
15 wt% $Sn_3O_4/BiVO_4$	28%	99%	0.040	0.992
10 wt% $Sn_3O_4/BiVO_4$	21%	72%	0.017	0.994
$BiVO_4$	18%	48%	0.007	0.990
Sn_3O_4	15%	34%	0.004	0.992
Blank	NA	10%	0.002	0.993

The reusability of photocatalysts during photocatalytic degradation plays a significant role in the application. Fig. 5a represents the re-usability of 15 wt% $Sn_3O_4/BiVO_4$ photocatalyst for the

photodegradation of RhB up to five runs, which reveals an indistinguishable degradation pattern in each run, confirming the higher stability of the photocatalyst. Unchanged pXRD pattern of the used photocatalyst after 5 cycles further confirms the stability of the 15 wt% $Sn_3O_4/BiVO_4$ photocatalyst (Fig.-5b).

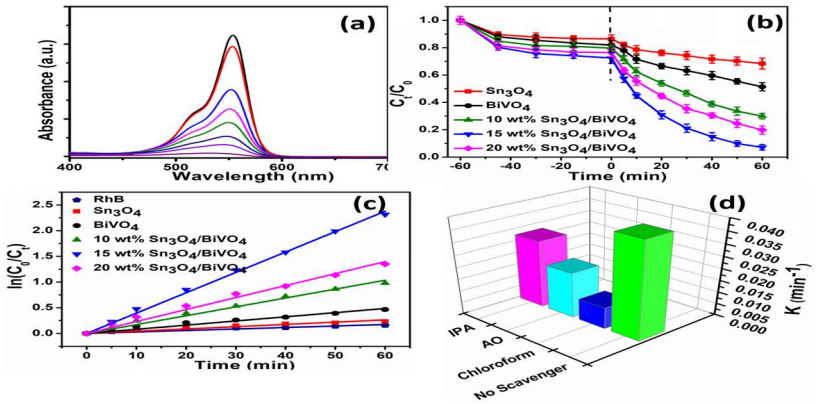

Fig.-3: (a) Absorption Spectrum of RhB Degradation, b-c) Degradation and Pseudo-First-Order Kinetic Plot RhB by Sn_3O_4, $BiVO_4$, and $Sn_3O_4/BiVO_4$ Nanocomposites, and d) Scavenger Studies

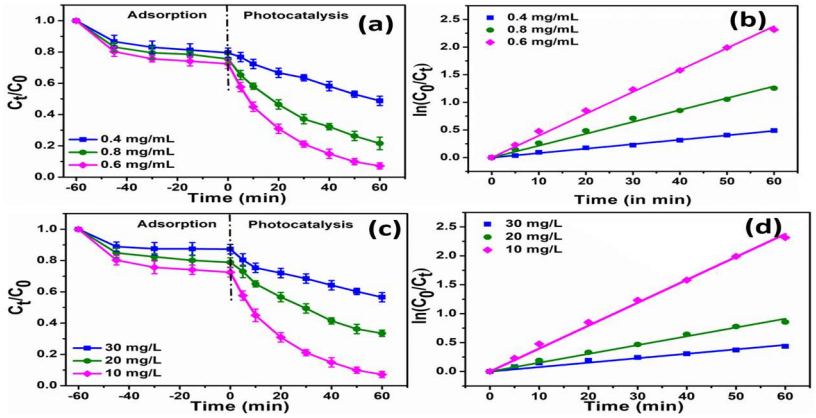

Fig.-4: a) Effect of Photocatalyst Dose on Performance of RhB Degradation, (b) Corresponding First-Order Kinetics Curves, (c) Effect of RhB Antibiotic Concentration on the Photocatalytic Performance, (d) Corresponding First-Order Kinetic Curves.

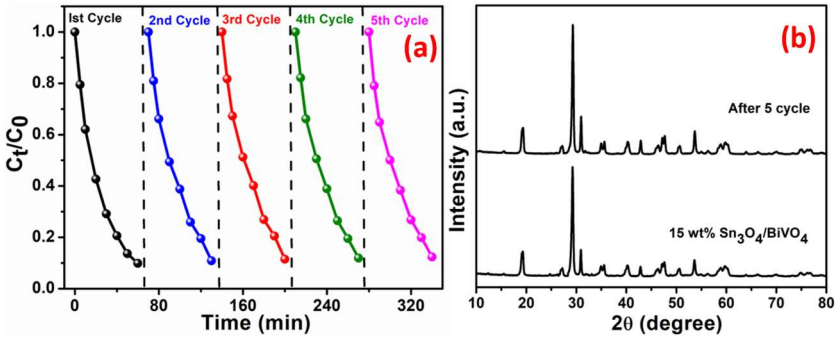

Fig.-5: (a) Recyclability Experiment; and (b) pXRD Plot of Pure and Used Photocatalyst

Photocatalytic Mechanism

The charge carrier route in a heterojunction-based photocatalyst is favored when the band positions of the respective semiconductors are suitably aligned. As the CB of Sn_3O_4 displays higher negative (-) potential as compared to $BiVO_4$, the e^- migrates from the CB of Sn_3O_4 to the EVB of $BiVO_4$, (type-II heterojunction system). The value of CB of $BiVO_4$ is at higher positive (+) potential than the $O_2^{-\bullet}$,(– 0.33 eV), that's why reduction of O_2 into a ($O_2^{-\bullet}$) by electron present in CB of $BiVO_4$ is quite difficult [23]. According to the radical trapping experiment, $O_2^{-\bullet}$ is one of the major active species that are responsible for the degradation of RhB,

which cannot be produced according to the type-II heterojunction mechanism (Fig.-6). The plausible mechanism (Z-scheme) was proposed for the degradation of RhB using $Sn_3O_4/BiVO_4$ heterojunction photocatalyst, as shown in Fig.-6. Sn_3O_4 and $BiVO_4$ both generate e^- and h^+ generated by absorption of visible light under exposure to sunlight. In $Sn_3O_4/BiVO_4$ heterojunction, the photo-generated electron in CB of $BiVO_4$ would move to VB of Sn_3O_4 to reconnect promptly with the photogenerated holes (h^+_{VB}), while the holes of $BiVO_4$ remain on it to oxidize RhB. Furthermore, the electron in the E_{CB} of Sn_3O_4 could effortlessly resettle to the O_2 molecules adsorbed over the surface $Sn_3O_4/BiVO_4$ heterojunctions to generate $O_2^{-\bullet}$ that oxidize RhB. The formation of superoxide radical anion ($O_2^{-\bullet}$) may take place from the two-electron process from hydrogen peroxide and by further reaction with holes, according to the following equations:[24]

$Sn_3O_4 + hv \longrightarrow$ electron + holes (1)

$BiVO_4 + hv \longrightarrow$ electron + holes (2)

$BiVO_4 + Sn_3O_4 \longrightarrow BiVO_4$ (electron) + Sn_3O_4 (holes) (3)

$BiVO_4$ (electron) + Sn_3O_4 (holes) $\longrightarrow$ Recombination (4)

$BiVO_4$ (holes) + $RhB_{(aq)} \longrightarrow CO_2 + H_2O$ (5)

Sn_3O_4 (electron) + $O_2 \longrightarrow Sn_3O_4 + O_2^{-\bullet}$ (6)

$O_2^{-\bullet} + RhB_{(aq)} \longrightarrow CO_2 + H_2O$

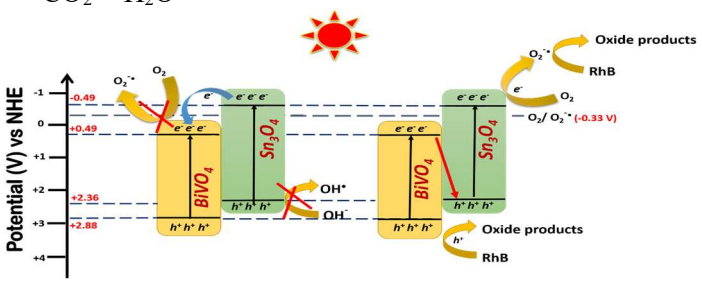

Fig.-6: Mechanism of RhB Degradation on $Sn_3O_4/BiVO_4$ Nanocomposite in Sunlight (a) Traditional type-II Heterojunction, (b) Z-Scheme Type

CONCLUSION

A novel $Sn_3O_4/BiVO_4$ heterogeneous photocatalyst was synthesized by the *in situ* hydrothermal method, which shows an excellent photocatalytic degradation activity towards RhB under exposure to sunlight. The photocatalytic degradation efficiency of the 15 wt% $Sn_3O_4/BiVO_4$ photocatalyst for RhB was much better than $BiVO_4$ photocatalyst, as the rate constant for RhB was about 6 times better in the case of 15 wt% $Sn_3O_4/BiVO_4$. The structural integrity and photocatalytic efficiency of $Sn_3O_4/BiVO_4$ nanocomposite remain unaffected after five runs.

ACKNOWLEDGMENTS

The authors are thankful to Prof (Dr). Rakesh Kumar Dwivedi (Dean), FoE, TMU, Moradabad, India, for his valuable insight and suggestions for completing this study.

CONFLICT OF INTERESTS

The authors declare that there is no conflict of interest.

AUTHOR CONTRIBUTIONS

All the authors contributed significantly to this manuscript, participated in reviewing/editing and approved the final draft for publication. The research profile of the authors can be verified from their ORCID ids, given below:

M. Farhan http://orchid.org/0009-0000-4775-7930
A.K. Singh http://orchid.org/0000-0003-2933-4058
G. Kumar http://orchid.org/0000-0003-0482-7024

REFERENCES

1. S. Sharma, A. Bhattacharya, *Applied Water Science,* **7(3)**,1043(2017), https://doi.org/10.1007/s13201-016-0455-7
2. F. Saadati, N. Keramati, M.M. Ghazi, *Critical Reviews in Environmental Science and Technology*, **46(8)**,757(2016), https://doi.org/10.1080/10643389.2016.1159093
3. S. Manzetti, R. Ghisi, *Marine Pollution Bulletin*, **79(1-2)**,7(2014), https://doi.org/10.1016/j.marpolbul.2014.01.005
4. R. Zhang, J. Tang, J. Li, Z. Cheng, C. Chaemfa, D. Liu, Q. Zheng, M. Song, C. Luo, G. Zhang, *Science of Total Environment*, **450-451**,197(2013), https://doi.org/10.1016/j.scitotenv.2013.02.024
5. J. Fick, H. Söderström, R.H. Lindberg, C. Phan, M. Tysklind, D.G.J. Larsson, *Environmental Toxicology and Chemistry*, **28(12)**, 2522(2009), https://doi.org//10.1897/09-073.1
6. I. Michael, L. Rizzo, C. S. McArdell, C. M. Manaia, C. Merlin, T. Schwartz, C. Dagot, D. Fatta Kassinos, *Water Reserve*,**47(3)**,957(2013), https://doi.org/10.1016/j.watres.2012.11.027
7. Q. T. Dinh, E. Moreau-Guigon, P. Labadie, F. Alliot, M. J. Teil, M. Blanchard, M. Chevreuil, *Chemosphere*,**168**,483(2017), https://doi.org/10.1016/j.chemosphere.2016.10.106
8. M. Z. Akbari, Y. Xu, Z. Lu, L. Peng, *Environmental Advances*, **5**, 100111(2021), https://doi.org/10.1016/j.envadv.2021.100111
9. M.J.F. Calvete, G. Piccirillo, C.S. Vinagreiro, M.M. Pereira, *Coordination Chemistry Reviews,* **395**, 63(2019), https://doi.org/10.1016/j.ccr.2019.05.004
10. J.C. Durán-Álvarez, E. Avella, R.M. Ramírez-Zamora, R. Zanella, *Catalysis Today*, **266**,175(2016), https://doi.org/10.1016/j.cattod.2015.07.033
11. M. Ge, L. Liu, Z. Zhou, *CrystEngComm,***14**,10381044(2012), https://doi.org/10.1039/c1ce06264f
12. A. Raja, P. Rajasekaran, K. Selvakumar, M. Arunpandian, K. Kaviyarasu, S.A. Bahadur, *Separation and purification Technology*,**233**, 115996(2020), https://doi.org/10.1016/j.seppur.2019.115996
13. W. Yin, W. Wang, L. Zhou, S. Sun, L. Zhang, *Journal of Hazardous Materials*, **173**,194(2010), https://doi.org/10.1016/j.jhazmat.2009.08.068
14. X. Chen, J. Zhou, Y. Chen, Y. Zhou, L. Ding, H. Liang, X. Li, *Process Safety and Environmental Protection,***145**, 364(2021), https://doi.org/10.1016/j.psep.2020.08.016
15. H. Jiang, H. Endo, H. Natori, M. Nagai, K. Kobayashi, *Materials Research Bulletin,* 44,700(2009), https://doi.org/10.1016/j.materresbull.2008.06.007
16. M. Long, W. Cai, J. Cai, B. Zhou, X. Chai, Y. Wu, *The Journal of Physical Chemistry B*, **110(41)**, 20211(2006), https://doi.org/10.1021/jp063441z
17. Q. Tang, X. Luo, S. Yang, Y. Xu, *Separation and purification Technology*, **248**,117039(2020), https://doi.org/10.1016/j.seppur.2020.117039
18. X. Luo, Z. Chen, S. Yang, Y. Xu, *Journal of Colloid and Interface Science*, **532**, 456(2018) https://doi.org/10.1016/j.jcis.2018.07.142
19. S. Chen, D. Huang, G. Zeng, W. Xue, L. Lei, P. Xu, *Chemical Engineering Journal*, **382**,122840(2020), https://doi.org/10.1016/j.cej.2019.122840
20. C. Li, S. Yu, H. Dong, C. Liu, H. Wu, H. Ce, G. Chen, *Applied Catalysis B: Environmental*, **238**, 284(2018), https://doi.org/10.1016/j.apcatb.2018.07.049
21. Y. Xu, M. Lv, H. Yang, Q. Chen, X. Liu, F. Wei, *RSC Advances*, **5**, 43473(2015), https://doi.org/10.1039/c4ra11383g
22. G. Kumar, *Journal of Inorganic & Organometallic Polymer Materials*, **33**, 2710(2023), https://doi.org/10.1007/s10904-023-02711-y
23. W.H. Koppenol, D.M. Stanbury, P.L. Bounds, *Free radical biology and medicine*, **49(3)**,317(2010), https://doi.org/10.1016/j.freeradbiomed.2010.04.011
24. M. Kowalkińska, P. Głuchowski, T. Swebocki, T. ossowski, A. Ostrowski, W. Bednarski, The *Journal of Physical Chemistry C*, **25(46)**, 25497(2021), https://doi.org/10.1021/acs.jpcc.1c06481

[RJC-9245/2025]